Alteration of Optical Properties in Polymer Materials under Low Earth Orbit (LEO) Space and Simulated Exposure

Elena A. Plis, Gregory Badura, Jainisha R. Shah, Heather M. Cowardin, Sydney Collman, Timothy R. Scott, Daniel P. Engelhart, and Ryan C. Hoffmann

***Abstract*— This paper provides an overview of the 16th Materials International Space Station Experiment (MISSE) project, conducted by a multiorganizational team of researchers. The orbital environment during the mission, including environmental sensors data and unexpected occurrences, are discussed. The research further examines the spectral changes in selected material, Kapton® TF, exposed to low Earth orbit conditions during the mission. Optical images of the material taken during the mission were analyzed using a machine learning approach. This process involved the use of a Radial Basis Function network to extract reflectance spectra from RGB/IR images. The findings were then compared with lab-based experiments of identical materials subjected to simulated space weather conditions. This comprehensive study aids in making accurate predictions about the performance of materials in space, thereby improving the reliability and safety of future space missions.**

***Index Terms*—Insulators; Space Radiation; Space Technology**

I. INTRODUCTION

The protection of satellites in the challenging space environment relies heavily on the characteristics of external spacecraft materials. These materials undergo continuous changes in their physical, chemical, and optical properties due to exposure to solar radiation and elements in Earth's upper atmosphere [1, 2]. Understanding how these material properties evolve over a mission's planned lifetime can enhance spacecraft reliability. Additionally, establishing correlation factors between actual space exposure and accelerated space weather experiments in ground facilities allows for more accurate predictions of on-orbit material performance through laboratory-based testing.

Low Earth orbit (LEO) is a particularly harsh environment for organic polymers because atomic oxygen (AO) is present along with all other environmental components [3]. There have been attempts by research teams in the U.S. and internationally to recreate the complex LEO conditions in ground-based facilities [e.g., 4, 5, 6]. However, there are significant differences between actual LEO exposure and simulated conditions on the ground. These differences include variations in AO quantum state and energy, temperature fluctuations, and exposure to both ultraviolet (UV) and ionizing radiation. Moreover, the effects of the space environment on spacecraft components depend on specific mission details, like mission duration, orbital parameters, spacecraft surface orientation to the sun, and alignment with the spacecraft velocity vector in LEO. Achieving integrated testing that precisely replicates actual space conditions is practically difficult within Earth-based testing facilities.

Hence, it's crucial to compare experiments conducted on Earth with the real exposure materials facing LEO. The Materials International Space Station Experiment Flight Facility (MISSE-FF) offers special testing capabilities for assessing new materials in the actual space environment [7]. By establishing correlation factors between real space exposure and accelerated space weather experiments, utilizing the MISSE-FF alongside simulated facilities becomes valuable. This approach allows for precise predictions of how materials will perform in orbit based on lab tests, ultimately enhancing the reliability and safety of space missions.

In our study, we delved into the effects of LEO on selected materials over both short and extended durations. We monitored how their spectral characteristics changed over time during the MISSE-16 mission. Identical material sets were exposed to LEO at ram, wake, and zenith ISS faces. To understand the impact of total irradiation dose and any flux-

This work was partically supported from the GTRI Independent Research and Development (IRAD) program, and the Air Force Office of Scientific Research, under the Remote Sensing and Imaging Physics Portfolio grant 20RVCOR024, led by Dr. Michael Yakes.

Elena A. Plis has joint appointment with Georgia Tech Research Institute (GTRI), Electro-Optical Systems Laboratory (EOSL), 430 10th Street NW, Atlanta, GA, 30318, USA (email: elena.plis@gtri.gatech.edu) and Assurance Technology Corporation, Carlisle, MA, 01741, USA (e-mail: plis@assurtech.com).

Gregory Badura is with Georgia Tech Research Institute (GTRI), Electro-Optical Systems Laboratory (EOSL), Atlanta, GA, 30318, USA, (e-mail: gregory.badura@gtri.gatech.edu).

Jainisha R. Shah and Ryan C. Hoffmann are with the Air Force Research Laboratory, Space Vehicles Directorate, USA, Kirtland AFB, Albuquerque, NM, 87117, USA (e-mail: afrl.rvborgmailbox@us.af.mil).

Heather M. Cowardin is with NASA Johnson Space Center, Orbital Debris Program Office, 2101 NASA Pkwy., Houston, TX 77058, USA (e-mail: heather.cowardin@nasa.gov).

Sydney Collman is with Assurance Technology Corporation (ATC), Carlisle, MA, 01741, USA (e-mail: collma@assurtech.com).

Timothy R. Scott is with DuPont de Nemours, Inc, Durham, NC 27703, USA (e-mail: tim.scott@dupont.com).

Daniel P. Engelhart is with University of New Mexico, Albuquerque, NM, 87131, USA (email: daniel.engelhart.unm@gmail.com).

dependent material responses, we took measurements alongside environmental data collected simultaneously. Optical images were transmitted to Earth shortly after these measurements. Upon initial analysis of the images, we employed a machine learning (ML) technique using a radial basis function (RBF) network to extract reflectance spectra from visible/infrared (IR) images. We then compared these findings with the results of lab-based irradiation experiments conducted on identical materials exposed to simulated space weather.

II. Experimental Details

A. Materials

Figure 1 presents the material selection for MISSE-16, encompassing various polymer classes, including the extensively studied Kapton® HN film serving as the reference material. Additionally, novel Kapton variations were included in the mission: CR (corona-resistant, crucial for shielding sensitive spacecraft equipment), CS (clear, smooth, and thermoformable, a potential alternative to traditional PI film in Multi-Layer Insulation blankets), WS (a possible substitute for traditional PI film in Multi-Layer Insulation blankets), XC (electrically conductive, significant for mitigating space charge on spacecraft), DR9 (conductive high-performance organic polymer), and TF (thermoformable, a prospective material for small satellite component manufacturing). This study provides a detailed discussion on Kapton® TF.

The study expanded its material selection to include two different Mylar variants, Melinex® 454 and Mylar® MO21, to evaluate their performance in LEO conditions, with a focus on enhancing multi-layer insulation efficiency. Additionally, the selection incorporated Zenite®, a Liquid Crystal Polymer (LCP) resin, and two hybrid materials, CORIN® XLS and Thermalbright® N, which combine Polyimide (PI) with Polyhedral Oligomeric Silsesquioxane (POSS). LCP films offer exceptional dimensional stability, fatigue, and creep resistance, along with high dielectric strength across a broad temperature range. PI/POSS materials have already been identified as excellent AO-resistant materials. A detailed study of their optical properties under different components of LEO space weather will be of great utility to the remote sensing community for the characterization of orbital debris and operational resident space objects (RSOs).

Lastly, Carbon Fiber Reinforced Polymer (CFRP, Economyplate™) and Glass Fiber Reinforced Polymer (GFRP, G-10/FR4 Glass Epoxy) represent advanced materials employed in contemporary LEO satellites. Nevertheless, laboratory data are scarce regarding their optical characteristics and possible degradation within the LEO environment. The rationale for including them in the MISSE-16 material selection was to establish a foundational understanding of their performance in the challenging LEO environment, utilizing optical monitoring to enhance space situational awareness.

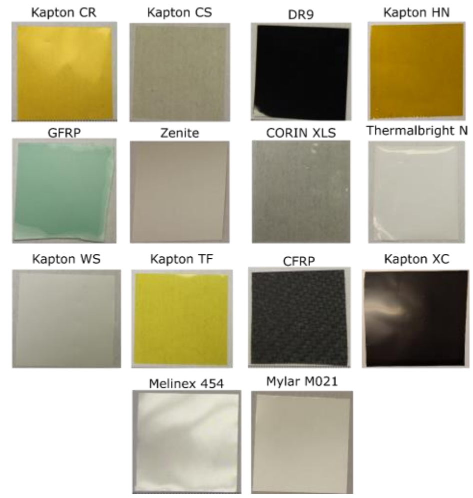

Figure 1. MISSE-16 material selection.

B. Overview of Space Experiment Details

During the course of the MISSE-16 mission, several unexpected occurrences were documented. On December 14, 2022, a coolant leak was detected on the Soyuz spacecraft that was docked at the MRM 1 (Nadir docking port). As of now, the precise cause of the leak remains undetermined. It is worth mentioning that the leak's trajectory was directed away from the MISSE-FF, thereby leaving the Material Science Carriers (MSCs) unaffected. A subsequent issue arose on February 3, 2023, when one of the samples began to detach from its holder on the MSC's swing side. In response to this, and to prevent potential Foreign Object Damage (FOD) in the International Space Station (ISS) environment, a strategic decision was made. The zenith 3 MSC was closed earlier than its counterparts—the ram 3 and wake 3 MSCs—to mitigate the risk. Finally, on February 11, 2023, another coolant leak (isooctane) occurred from the Russian Progress spacecraft. The Progress spacecraft was located at MRM 2 (Poisk) docking port and it appeared that the leak direction was away from MISSE-FF. The exposure times in the LEO for each MSC with our payload were 193 days for the wake 3 slot, 173 days for the zenith 3 slot, and 183 days for the ram 3 slot.

The UV dose D (J/cm^2) obtained by the swing and mount sides of each MSC was calculated as a product of measured UV intensity I (W/cm^2) and exposure time (seconds), as summarized in Fig. 2. While it was initially believed that the zenith side of the ISS, which faces the sun, would receive the greatest amount of UV radiation, a closer look at the UV data (as shown in Figure 2) paints a different picture. Surprisingly, it appears that the ram face of the ISS, the side moving forward in its orbit, receives the majority of the UV radiation.

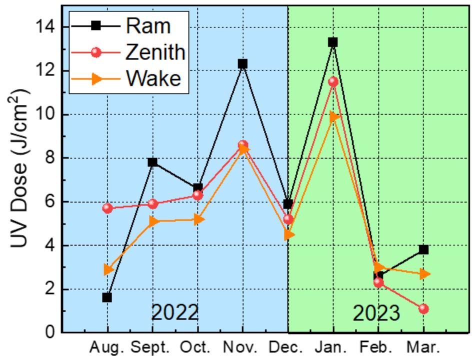

Figure 2. UV dose received by MSCs at different ISS faces.

Temperature changes that the MSCs experienced during the mission are summarized in Figure 3. The lowest temperature recorded was -34.3°C in December 2022 on the swing side of the MSC on the wake face of the ISS. The highest temperature, on the other hand, was 44.8°C in October 2022 on the swing side of the MSC on the zenith face of the ISS.

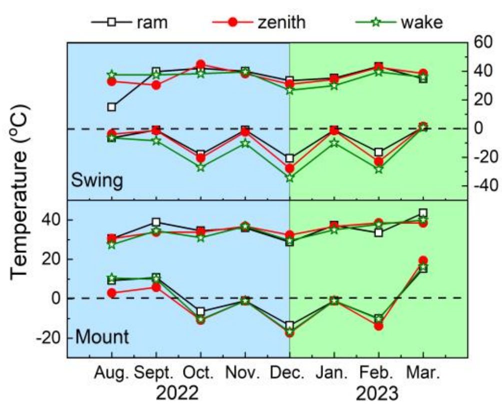

Figure 3. Min and max temperature of swing and mount sides of MSCs at ram, zenith, and wake ISS faces.

The total AO fluence experienced by each MSC was 1.6 x 10^{19} atoms/cm^2 (wake), 7.01 x 10^{18} atoms/cm^2 (zenith), and 3.07 x 10^{20} atoms/cm^2 (ram). AO fluence was determined using the mass loss technique based on dehydrated mass measurements before and after flight [5]. The Kapton witness sample on each MSC had an exposed area of 4.661 cm^2.

Upon reviewing the radiation data for MISSE-16, the Aegis Aerospace operations team observed that the data may have been affected by noise in the active radiation sensor. Consequently, the team has decided to use the passive dosimeter from Landauer (Luxel+ PA dosimeters and the units are in mrem). The Luxel+ PA samples were stored below the sample tray, inside the MSC. The power radiation sensor was also utilized for the characterization of the LEO environment, however, the results were inconclusive. The deep dose equivalent (DDE) electron irradiation dose received by each MSC was 1.8 x 10^4 mrem (wake), 1.5 x 10^4 mrem (zenith), and 1.2 x 10^4 mrem (ram).

The imaging cadence for the MISSE-16 samples was designed to capture the most accurate representation of their behavior over time. This was planned as follows: for the initial 7 days, daily images in the visible and infrared (IR) range of each sample were taken. Following this intensive first week, the frequency of imaging was reduced for the subsequent two months, with weekly images of each sample being taken. For the remainder of the mission's duration, the imaging was scheduled to occur on a monthly basis. This tiered approach to imaging was aimed at providing detailed insights during the initial critical phase and continuing with regular updates throughout the mission.

C. Micrometeoroids and Orbital Debris (MMOD) Impact

Post-flight analysis was carried out aimed at detecting micrometeoroids and orbital debris (MMOD) impacts on the MSCs. This procedure was executed by the NASA Hypervelocity Impact Technology (HVIT) Team at the Aegis Aerospace facility located in Webster, Texas. The primary objective of this analysis was to identify and measure craters with a diameter exceeding 0.5 mm. Inspection was restricted to the exterior surfaces of the MSCs, specifically those that were devoid of experimental or sample materials. The inspection on the experimental/sample side was separately conducted during the materials de-integration process by the MISSE-16 Principal Investigator (PI) and Co-PI.

D. Flight-duplicates Preparation

Material irradiation with high-energy electrons as well as the Vacuum UV (VUV) exposure was performed in the Jumbo space irradiation chamber at the Spacecraft Charging and Instrument Calibration Laboratory (SCICL) at Kirtland Air Force Research Laboratory [8]. Materials were bombarded with high-energy (100 keV) electrons produced by a mono-energetic Kimball Physics EG8105-UD electron flood gun. The maximum electron fluence the materials under investigation were exposed to is 8.5 x 10^{13} electrons/cm^2. A 24-h vacuum dehydration bakeout was performed on all samples at 60° C prior to radiation exposure to remove any absorbed water. Details of the electron irradiation procedure are reported elsewhere [9].

The space-simulated VUV exposure was conducted using three Resonance KrLM-LQD12 lamps installed in the Jumbo chamber at SCICL. The lamp spectrum is composed of 1.0 parts and 2.38 parts of photons with peak wavelengths at 116.5 nm and 123.6 nm, respectively [10]. The photon flux at each wavelength was estimated as 5.5 x 10^{20} photons/ (seconds · cm^2 · A) at 116.5 nm and 1.06 x 10^{20} photons/ (seconds · cm^2 · A) at 123.6 nm. Based on Lyman-Alpha flux in-vacuum conversion [11], samples receive an average of 50.9 equivalent sun hours (ESH) per single sample carousel rotation. The expected solar net flux for 6 months of the MISSE-16 mission was calculated to be ~1094 ESH, assuming that ISS completes approximately sixteen 90-minute revolutions per day. The Python code was generated to calculate the angle of each sample relative to the sun according to the orbital beta-angle and ISS position along the orbit.

Exposure testing of sample materials to an 8 km/s oxygen atom beam was conducted according to ASTM-E2089-

15A using the FAST™ source at the Physical Sciences Inc. The effective peak atomic oxygen fluence during the exposure was calculated using the known witness sample density (Kapton© H, 1.427g/cm^3) and LEO erosion yield of the same material (3 x 10^{-24} cm^3/O-atom). Effective peak atomic oxygen fluence during the run was 3.1×10^{20} O-atom/cm^2 which corresponds to 6 weeks of LEO exposure. Before exposure, all samples were stored in the vacuum chamber for 24 hours to remove water. They were then evacuated and weighed over time to monitor water absorption and allow for the dry mass calculation. Details of the AO-irradiation procedure may be found in [12].

E. *Optical Properties Characterization*

The Basler daA1600 camera was utilized to sequentially capture visible and IR images of every sample on the MSCs mounted on the zenith, ram, and wake faces of the ISS. Upon completion of each measurement, orbital images were transmitted to Earth for analysis. Subsequently, a ML approach, utilizing an RBF network [13], was employed to extract reflectance spectra from the visible/IR images. Once retrieved from the on-orbit MISSE-FF cameras, red-green-blue (RGB) data from non-over-saturated regions, under both visible and IR lighting conditions, were selected for analysis. These pixel counts were then white-balanced in accordance with the scene context, a feasible adjustment due to the uniform settings implemented in both the flight and ground cameras. The MISSE-FF data in visible wavelength range were subsequently transformed into the CIELAB color space [14] and inputted into the RBF network. The application of the ML algorithm resulted in the generation of an estimated reflectance spectrum for each image.

Directional Hemispherical Reflectance (DHR) measurements were conducted at regular intervals both during the electron bombardment and the VUV exposure using a Spectral Evolutions Inc. spectrometer (model SR-3501), in tandem with a Tungsten halogen light source from Ocean Insight (model HL-2000-FHSA) installed in the Jumbo space irradiation chamber. The procedure for data collection commenced with the measurement of white and black standards, specifically Spectralon® and Acktar Black®, using a Spectralon® integrating sphere mounted on a robotic arm. The in-depth details of the DHR optical measurements have been previously reported elsewhere [15]. During the DHR measurement process, the electron beam or UV exposure was turned off to prevent damage to the Spectralon standard.

For samples exposed to AO, *in situ* DHR measurements were not feasible. Instead, post AO exposure, these materials were transferred to the Jumbo chamber, along with their pristine (unexposed) counterparts. The DHR measurements were then conducted under vacuum conditions, following the same procedure.

III. RESULTS

Figure 4 presents visible and IR images captured during the MISSE-16 mission. The initial measurements, serving as the pristine baseline, were taken on the first day of exposure. While the measurements were conducted according to the cadence detailed in the "Experimental Details B. Overview of Space Experiment Details", we have chosen to present only specific data sets for clarity: images taken at the end of the first week and subsequently, at the end of every month of the mission. The IR images were obtained using the same camera, with IR LEDs acting as the source of illumination.

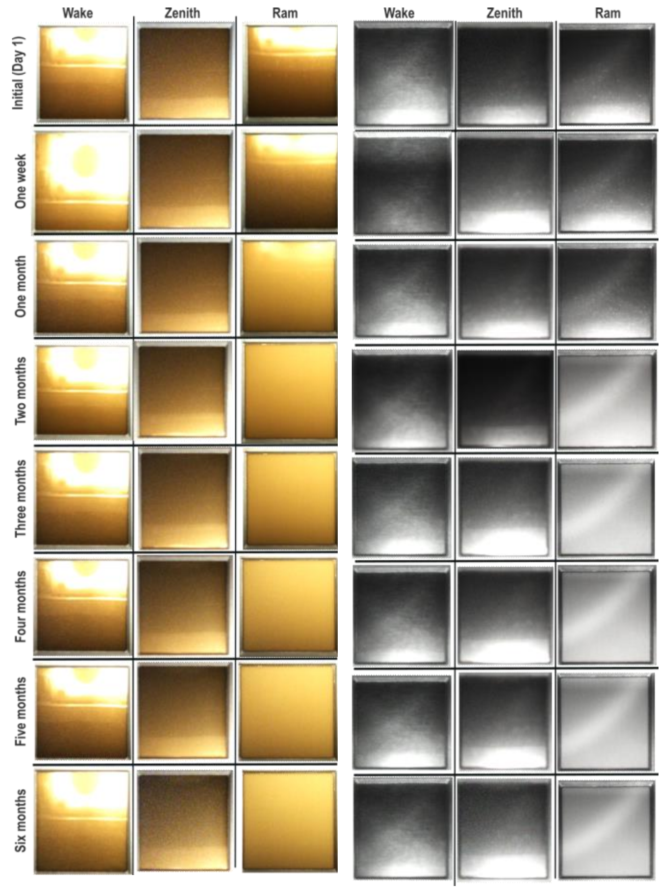

Figure 4. Visible and IR images of Kapton® TF taken during the MISSE-16 mission.

Figure 5 presents representative results from the MMOD inspection. It is important to note that no signs of MMOD impacts were detected on the experimental/sample side of the MSCs. However, seven instances of MMOD were identified on the MSCs allocated for our payload. A detailed summary of these MMOD impacts can be found in Table 1.

Table 1. Results of Post-flight MMOD Inspection

Slot location	# of craters	Equivalent diameter (mm)	Depth (mm)
Ram 3	3	0.61 – 0.88	0.21 – 0.39
Zenith 3	3	0.34 – 0.52	0.17 – 0.36
Wake 3	1	0.82	0.41

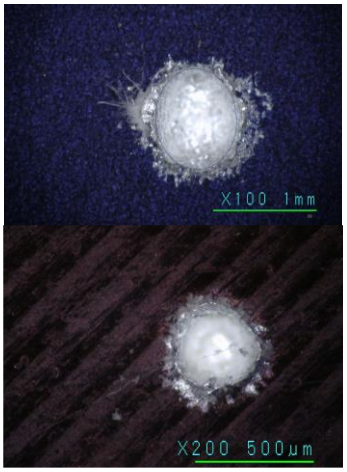

Figure 5. Representative results of MMOD inspection.

Figure 6 illustrates the alteration in coloration of Kapton® TF material subjected to the LEO space environment on the wake, zenith, and ram faces of the ISS. This transformation occurred over approximately six months of the MISSE-16 mission. Photographs were captured four weeks after the payload's return to Earth, so some restoration of space-weather induced damage is expected, especially for wake material. The peripheral area of each sample remained unexposed to the space environment, being shielded by the aluminum frame of MISSE-FF during the process of material integration.

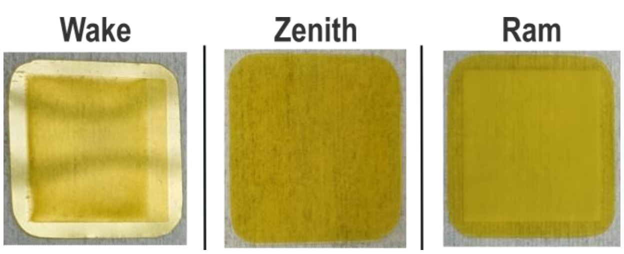

Figure 6. Photographs of Kapton® TF material exposed to LEO space environment at wake, zenith, and ram faces of ISS after ~6 months of MISSE-16 mission.

Figure 7 presents the correlation between reflectance values predicted by machine-learning algorithms using orbital data and those measured on the ground for flight-duplicate samples. The top panel illustrates the wake face of the ISS juxtaposed with high-energy electron exposure on the ground. The middle panel corresponds to the zenith face of the ISS alongside ground-based VUV exposure. The bottom panel represents the ram face of the ISS compared with AO exposure on the ground.

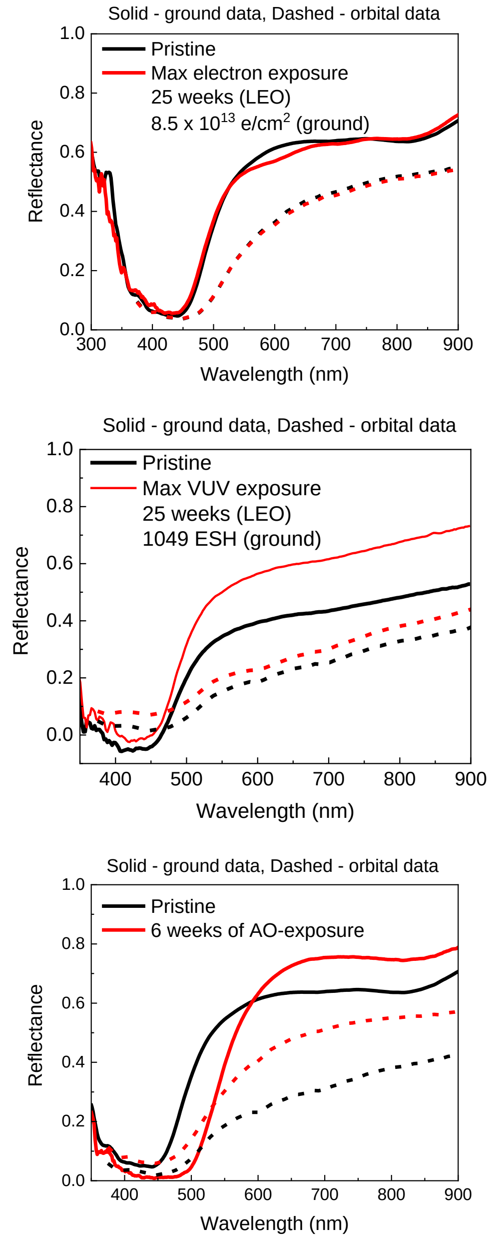

Figure 7. Correlation between ML-predicted using orbital date and ground-measured reflectance values for flight-duplicate samples. The top panel presents a comparison between the wake face of the ISS and the high-energy electron exposure on Earth. The middle panel parallels the zenith face of the ISS with the ground-based VUV exposure. Lastly, the bottom panel demonstrates the relationship between the ram face of the ISS and AO exposure experienced during ground-based AO exposure.

IV. Discussion

The notable changes in optical properties of Kapton® TF occur during the AO exposure at the ram face of the ISS (Figure 4). A specular reflection of the illumination source (LED) gradually becomes more diffuse and after one month in orbit, no reflection is observed. Interactions of high-energy electron and solar photons predominant at the wake and zenith faces of the ISS resulted in only minimal modifications to the samples. IR imaging corroborated this trend - the wake and zenith samples displayed no substantial changes. However, the grayscale of the ram image sequence lightened, indicating a possible transformation in the surface properties of the Kapton® TF.

The findings are consistent with the examination results of the returned materials, as depicted in Figure 6. The area of the ram sample exposed to space underwent a substantial color shift in contrast to the area shielded by the metal frame. This change, from a shiny to a dull surface, suggests considerable roughening of the exposed section. The wake sample kept its reflective property but became less transparent. In the case of the zenith sample, no discernible chromatic differentiation was observed between the exposed and frame-protected sections.

The MMOD inspection of all MISSE-16 materials and the metal frame surrounding them, carried out during the disassembly of returned materials, found no evidence of micrometeoroid impacts. This was expected since IR images, an effective tool for identifying any mechanical damage caused by the space environment, such as scratches, holes, craters, tears, etc., did not display any of those.

The objective of the MMOD inspection carried out by the NASA HVIT team was to identify all potential MMOD impacts/features on the MSCs using a 0.5 mm threshold for further examination. Although many features were identified below this threshold, they were noted in the internal report, but not further analyzed for this evaluation. There were smaller craters identified, but were not fully characterized. The eleven MMOD indications were discovered on the exterior surfaces of MSCs carrying our payload. It should be noted that studied MSCs have flown more than once, and damage may not have occurred specifically during the MISSE-16.

The comparison between the reflectance signal predicted by the ML algorithm using the visible and IR camera images, and the corresponding flight duplicates, demonstrates a strong qualitative correlation, as illustrated in Figure 7. The reflectance value remained relatively stable under high-energy electron exposure conducted in the Jumbo irradiation chamber. The Kapton® TF sample, having been exposed to 1049 equivalent sun hours (ESH) in the Jumbo chamber, exhibited increased reflectivity, akin to the same material exposed to the solar photons at the zenith face of ISS during the 26 weeks of the MISSE-16 mission. Furthermore, both space and ground-based AO exposure resulted in the material becoming more reflective. It is important to note that on the ground, we only performed 6 weeks of LEO-equivalent exposure. Hence, for comparison, data from 6 weeks of ZO exposure at the ram face of the ISS were utilized.

The quantitative divergence between the space and ground data may be ascribed to a few factors. Primarily, the measurements were conducted using different setups. For a more precise comparison, we plan to execute the image-capturing process of electron- and VUV-exposed materials using a camera and light board identical to those installed in the MISSE-16 at the Jumbo chamber, and subsequently examine the results generated by the ML algorithm.

Subsequently, it's crucial to enhance the ML model to account for specular scattering. Currently, its functioning is largely dependent on diffuse reflectance. Furthermore, the issue of white balancing poses a significant challenge and is a source of potential errors. It has been particularly problematic due to the oversaturation issues we dealt with during the image cadence execution.

Lastly, the inherent discrepancies between ground and space experiments must be factored in. Predominantly, space experiments encompass a synergistic interaction of all LEO environmental factors, even when we attribute the predominant effect to a specific LEO environment. On the other hand, our ground-based aging experiment subjected samples to each degrading agent independently. To align more closely with space aging, we need to enhance our ground aging capabilities to account for the interaction of multiple space weather components.

In essence, space experiments are conducted in a complex environment where various factors work in concert. This synergistic effect can lead to different outcomes compared to when each factor is tested individually, as we have done in our ground-based experiments. Therefore, to emulate the conditions in space more accurately, it would be beneficial to develop a ground-based testing environment where multiple space weather components can interact simultaneously. This would not only provide more accurate data but also provide a better understanding of the interactions between different environmental factors and their combined effect on the materials.

V. Conclusion

In conclusion, the study has revealed some insights into the optical property changes of Kapton® TF when subjected to various space weather components. The most significant changes were observed at the ram-exposed material, which demonstrated a transition from specular to diffuse reflection, alongside substantial color shifts and surface roughening. On the contrary, minimal modifications were observed in samples subjected to high-energy electron and solar photon interactions, predominant at the wake and zenith faces of the ISS.

The study also found no evidence of micrometeoroid impacts, aligning with expectations based on the absence of mechanical damage in the IR images.

The ML algorithm's predictions showed a strong qualitative correlation with the actual reflectance values obtained from both space and ground experiments, despite the quantitative discrepancies. These discrepancies might be attributed to inherent differences between space and ground experiments. Therefore, future work will aim to align the ground-based experimental setup more closely with space conditions and enhance the ML model's capabilities to account for specular scattering and address issues related to white balancing.

Furthermore, the study underscores the necessity to account for the synergistic effect of all LEO environmental factors in space experiments. Emulating these conditions in ground-based experiments could provide more accurate data and a better understanding of the interactions between different environmental factors and their combined effect on the materials.

VI. Public Release Clearance

The views expressed are those of the author and do not necessarily reflect the official policy or position of the Department of the Air Force, the Department of Defense, or the U.S. government. The appearance of external hyperlinks does not constitute an endorsement by the United States Department of Defense (DoD) of the linked websites, or the information, products, or services contained therein. The DoD does not exercise any editorial, security, or other control over the information you may find at these locations.

Trade names and trademarks are used in this report for identification only. Their usage does not constitute an official endorsement, either expressed or implied, by the National Aeronautics and Space Administration. Approved for public release; distribution is unlimited. Public Affairs release approval #

VII. Acknowledgements

We express our gratitude to DuPont de Nemours for generously providing all the materials needed for our research. Our heartfelt appreciation goes to the AEGIS Aerospace team, whose invaluable contributions have been instrumental in the successful execution of the MISSE-16 orbital experiments. We also wish to acknowledge Eric Christiansen, Heather Cowardin, and Jim Hyde for their diligent efforts in performing the MMOD examination on the exterior surfaces of the MSCs.

-

[1] E. Grossman, I. Gouzman I. Space environment effects on polymers in low earth orbit. Nucl. Instrum. 208:48-57 (2003)

[2] Y. Lu, Q. Shao, H. Yue, F. Yang. A review of the space environment effects on spacecraft in different orbits. IEEE Access 7: 93473–93488 (2019)

[3] K. K. De Groh, A. B. Banks (2019). Atomic oxygen erosion data from the MISSE 2–8 Missions, NASA/TM-219982. https://ntrs.nasa.gov/search.jsp

[4] H. N. Yeritsyan, A. A. Sahakyan, N. E. Grigoryan, V. V. Harutyunyan, V. V. Arzumanyan, V. M. Tsakanov, B. A. Grigoryan, H. D. Davtyan, V. S. Dekhtiarov, C. J. Rhodes, I. G. Assovsky. Space low earth orbit environment simulator for ground testing materials and devices. Acta Astronautica 181:594-601 (2021)

[5] C. A. Maldonado, A. D. Ketsdever, J. D. Williams. A Magnetically Filtered Atomic Oxygen Plasma Source for Low-Earth-Orbit Simulation. J Spacecraft Rockets. 58(5):1406-15 (2021)

[6] C. T. Smith, M. Delkowki, J. V. Anguita, D. C. Cox, C. Haas, S. R. Silva. Complete atomic oxygen and UV protection for polymer and composite materials in a low earth orbit. ACS Applied Materials & Interfaces 13(5):6670-7 (2021)

[7] K. K. deGroh, D. A. Jaworske, G. Pippin, P. P. Jenkins, R. J. Walters, S. A. Thibeault, I. Palusinski, J. R. Lorentzen. Materials international space station experiment (misse): overview, accomplishments and future needs. In Annual International Space Station Research and Development Conference 2014 Jun 17 (No. GRC-E-DAA-TN15048).

[8] Cooper, R., and Hoffman, R. 2015. Jumbo space environment simulation and spacecraft charging chamber characterization," Tech. rep., Air Force Research Laboratory, Space Vehicles Directorate Kirtland AFB.

[9] Engelhart, D. P., Plis, E., Humagain, S., Greenbaum, S., Ferguson, D., Cooper, R., and Hoffmann, R. 2017. Chemical and electrical dynamics of polyimide film damaged by electron radiation. *IEEE Trans. Plasma Sci*. 45 (9): 2573–2577.

[10] Resonance KrLM-LQD12 lamp brochure. Available at: https://resonance.on.ca/index_htm_files/LampComparisonBrochure.pdf

[11] Lean J. L., Skumanich A. 1983. Variability of the Lyman alpha flux with solar activity. *J. Geophys. Res*. 88(A7): 5751-5759.

[12] Plis, E., Bengtson, M., Engelhart, D. P., Badura, G., Scott, T., Cowardin, H., Reyes, J., Hoffmann, R., Sokolovskiy, A., Ferguson, D. C., Shah, J., Horne, S. 2022. Characterization of novel spacecraft materials under high energy electron and atomic oxygen exposure. In *AIAA SCITECH 2022 Forum*, p. 0797.

[13] R. M. Nguyen, D. K. Prasad, M. S. Brown.Training-based spectral reconstruction from a single RGB image. In European Conference on Comp. Vis. 186-201 (2014)

[14] Luo, M.R. (2015). CIELAB. In: Luo, R. (eds) Encyclopedia of Color Science and Technology. Springer, Berlin, Heidelberg.

[15] M. Bengtson, J. Maxwell, R. Hoffman, R. Cooper, S. Schieffer, D. Ferguson, H. Cowardin, E. Plis, D. Engelhart. "Optical Characterization of Commonly Used Thermal Control Spacecraft Paints in a Simulated GEO Environment". Advanced Maui Optical and Space Surveillance Technologies Conference, Maui, USA, September 2018